

# RADIATION PRESSURE FORCE AND BLACK HOLE MASS DETERMINATION IN LOW REDSHIFT TYPE-I AND TYPE-II ACTIVE GALACTIC NUCLEI

HAGAI NETZER,<sup>1</sup>

*Draft version October 28, 2018*

## ABSTRACT

The distributions of  $L([\text{O III}]\lambda 5007)$ , black hole (BH) mass and  $L/L_{\text{Edd}}$  in two large samples of type-I and type-II active galactic nuclei (AGNs) are compared in order to test the suggestion that radiation pressure force is affecting the gas velocity in the broad line region and hence the BH mass determination. The samples are drawn from the SDSS archive and are modified to represent the same parent distribution at  $0.1 \leq z \leq 0.2$ . BH masses in type-I sources are calculated in two different ways, one using a simple virial mass assumption and the other by taking into account the effect of radiation pressure force on the gas. The simple virial mass estimate results in good agreement with the  $\sigma_*$ -based BH mass and  $L/L_{\text{Edd}}$  estimates in type-II sources. In contrast, there is a clear disagreement in the  $L/L_{\text{Edd}}$  distributions when radiation pressure-based estimates are used. This indicates that radiation pressure force is not important in  $0.1 \leq z \leq 0.2$  AGNs with  $L_{5100} = 10^{42.8-44.8}$  ergs s<sup>-1</sup>. This has important implications to the physics of the gas producing the broad emission lines in AGNs, in particular the existence of extremely large column density ( $\sim 10^{24}$  cm<sup>-2</sup>) clouds.

*Subject headings:* Galaxies: Active – Galaxies: Black holes – Galaxies: Nuclei – Galaxies: Quasars: Emission Lines

## 1. INTRODUCTION

Black hole (BH) masses in thousands of type-I active galactic nuclei (AGNs) can now be obtained by combining measurements and understanding of the gas in the broad line region (BLR) of such sources. Information on the gas kinematics in the BLR is obtained from the study of emission line profiles which leads to the conclusion that, in many sources, the motion is virialized and completely dominated by the BH gravity (e.g. Onken and Peterson 2002). This provides a simple way of estimating the mean Keplerian motion of the gas e.g. from measured FWHMs of broad emission lines. Size measurements of the BLR are the result of reverberation mapping (RM) in a small ( $\sim 35$ ) number of low redshift ( $z < 0.3$ ) AGNs. This provides a scaling relationship between the BLR size and the source luminosity. The combination of BLR size and mean gas velocity is the basis for the so-called “virial” (or “single epoch”) method (Vestergaard and Peterson 2006 and references therein) for obtaining BH masses ( $M_{\text{BH}}$ ) from spectroscopic observations of type-I AGNs.

The accuracy of the virial method depends on various assumptions about the RM method, the source luminosity and the line profiles. Detailed discussion of RM and its limitations, and listing of the available data, are given in Kaspi et al. (2000, hereafter K00) and Kaspi et al. (2005; hereafter K05). Improvements and additions to the K00 sample are described in Bentz et al. (2008; hereafter B08) where full account of the host galaxy contribution to the observed flux is included. Errors and uncertainties are discussed in Peterson and Bentz (2006) and various other publications and are estimated to be a factor of  $\sim 2$  on  $M_{\text{BH}}$ . This is a combination of the uncertain host galaxy flux in low luminosity AGNs, the

uncertainties on the measured time lags, and uncertainties in the conversion of observed broad line profiles (in this work  $\text{FWHM}(\text{H}\beta)$ ) to a “mean gas velocity”.

An important recent development is the suggestion by Marconi et al. (2008; hereafter M08) that radiation pressure force operating on the BLR gas can play an important role in determining the gas dynamics. Such force results in a reduced effective gravity which is translated to a larger  $M_{\text{BH}}$  for a given observed FWHM. The treatment of radiation pressure depends on the assumed gas distribution in the BLR. It is straightforward in the case of the “cloud model” where the gas is assumed to be distributed in large column density condensations (clouds) or filaments (e.g. Netzer 1990 and references therein). It is more complicated in other models e.g. the “locally optimally emitting clouds (LOCs)” scenario (Baldwin et al. 1995; Korista et al. 1997) where many different components with different density, column density and level of ionization occupy the same volume of space. The M08 suggestion is not relevant to those models where the material is assumed to be driven away from a central disk in form of a clumpy wind (e.g. Everett 2005; Elitzur & Shlosman 2006). In such cases the virial assumption breaks down and the line profiles cannot be used in the estimate of  $M_{\text{BH}}$ . In the following I will only consider the cloud model which is the focus of the M08 paper.

The effect of radiation pressure force is most noticeable in high luminosity sources where the radiation pressure acceleration can be very large. This is illustrated in the recent analysis by Marconi et al. (2008b) who applied their corrected (i.e. after applying the radiation pressure force term, see below) mass estimates to the large AGN sample of Shen et al. (2008). A clear signature of the correction is seen in the distribution of the normalized accretion rate,  $L/L_{\text{Edd}}$ , which is narrower and hardly ever exceeds 0.1 (Marconi et al. 2008b Fig.1). In contrast, the simple virial method results in a substantial fraction

<sup>1</sup> School of Physics and Astronomy and the Wise Observatory, The Raymond and Beverly Sackler Faculty of Exact Sciences, Tel-Aviv University, Tel-Aviv 69978, Israel

of sources with  $L/L_{\text{Edd}} \simeq 1$ .

This paper proposes a novel method to test the M08 suggestion by comparing two large samples of type-I and type-II AGNs drawn from the Sloan Digital Sky Survey (SDSS; York et al. 2000). The assumption that the two are drawn from the same parent distribution enables the comparison of BH masses that are obtained by two independent methods. This provides a direct test of the importance of radiation pressure force in accelerating the BLR gas. In §2 I describe the two samples and their selection. §3 compares the mass and accretion rate distributions and contrast them with the M08 suggestion. Finally, §4 gives a short discussion of the uncertainties and the implications to higher redshift higher luminosity AGNs.

## 2. BLACK HOLE MASS AND ACCRETION RATE DISTRIBUTIONS

### 2.1. Low redshift type-I and type-II AGN samples

The present work is based on the analysis of two samples of type-I and type-II AGNs that cover the same range in redshift and luminosity. The type-I sample is the one described in Netzer and Trakhtenbrodt (2007; hereafter NT07). It includes all SDSS Data Release Five (DR5) type-I AGNs with  $z \leq 0.75$ . The redshift limit is dictated by the need to measure the broad  $H\beta$  line, the optical continuum luminosity ( $\lambda L_\lambda$  at 5100Å; hereafter  $L_{5100}$ ) and the  $[\text{O III}] \lambda 5007$  narrow emission line in the SDSS spectra. The extraction, line and continuum fitting, and luminosity and  $M_{\text{BH}}$  determinations are explained in NT07. The values of  $L_{5100}$  and  $M_{\text{BH}}$  are very similar to the ones listed in the recent compilation of Shen et al. (2008). Radio loud (RL) AGNs are excluded from the present work (see below) but their inclusion changes nothing in the type-I type-II comparison.

The type-II sample is an extension of the SDSS/DR1 sample discussed in Kauffmann et al. (2003) and Heckman et al. (2004). It is based on the DR4 release (Adelman-McCarthy et al., 2006) and is publicly available on the MPA site<sup>2</sup>. For each source it includes redshift, stellar velocity dispersion measured through the 3'' SDSS fiber,  $L([\text{O III}] \lambda 5007)$  with and without reddening correction,  $L([\text{O III}])/L(H\beta)$ ,  $L([\text{N II}])/L(H\alpha)$  and various other properties that are not relevant to the present work.

The above two samples are different in two major ways:

**1. AGN type:** While the type-I sample includes only broad line AGNs, the type-II sample contains both high excitation (Seyfert and QSO) and low excitation line (LINER) AGNs (starburst galaxies have been removed using standard line ratio diagrams; see Kauffmann et al. 2003). It is therefore important to identify similar ionization and excitation ranges and to remove the LINERs from the type-II sample prior to the comparison. The separation is done by applying two criteria:  $L([\text{O III}])/L(H\beta) > 1.4$  (the lowest value in the NT07 sample) and

$$\log L([\text{N II}])/L(H\alpha) \leq \log L([\text{O III}])/L(H\beta) - 0.4. \quad (1)$$

The resulting type-II sub-sample is in good agreement with other work of this type (e.g. Kauffmann et al. 2003;

Groves et al. 2006) and its mean excitation level is in agreement with the NT07 sample.

**2. Flux limit and redshift distribution:** While the original type-II sample of Kauffmann et al. (2003) and Heckman et al. (2004) is selected from the flux limited SDSS galaxy sample, the extended DR4 catalog used here is defined in a different way and includes all sources classified as galaxies. These are further classified according to the emission line intensities, in particular  $[\text{O III}] \lambda 5007$ . This selection reaches very low  $L([\text{O III}] \lambda 5007)$  at low redshift. The type-I selection is a combination of SDSS colors in a flux limited ( $i=19.1$  mag) sample and the detection of broad emission lines. This results in a noticeable difference between low and high redshift sources. For high redshift type-I sources that are dominated by the AGN continuum, the flux limit is the determining factor. For low redshifts low luminosity AGNs, contamination by the host galaxy makes the detection of broad emission lines more difficult and, in many cases, becomes the limiting selection factor. Inspection of the  $L_{5100}$  distribution in the NT07 sample suggests that the detection of broad emission lines is the limiting factor for all  $z \leq 0.1$  AGNs. This corresponds to  $L_{5100} \simeq 10^{42.8}$  ergs  $\text{s}^{-1}$  for the faintest sources at  $z = 0.1$ . For  $z \geq 0.15$ , the distribution of  $L_{5100}$  is consistent with the flux limit of the sample. Thus, at  $z \sim 0.1$ , the type-II sample is deeper in terms of  $L([\text{O III}] \lambda 5007)$  and the type-I sample is incomplete.

The distribution of  $L([\text{O III}] \lambda 5007)$  in type-I AGNs was studied in various papers including Kauffmann et al (2003), Zakamska et al. (2003) and Netzer et al. (2006). The space distribution of all AGNs, based on  $L([\text{O III}] \lambda 5007)$ , is studied in other recent publications (Reyes et al. 2008 and references therein). Netzer et al. (2006) show a weak dependence of  $L([\text{O III}] \lambda 5007)/L_{5100}$  on redshift and a stronger dependence on  $L_{5100}$  within different redshift intervals. For  $z \sim 0.1$ , the mean and the median values in the NT07 sample are similar and suggest  $L_{5100}/L([\text{O III}] \lambda 5007) \simeq 340$ . This ratio, which is not corrected for reddening (see below), is assumed to represent all sources in the present work.

To produce two samples that are compatible in redshift and in  $L([\text{O III}] \lambda 5007)$ , I chose a flux limit for the type-II sources that corresponds to  $L_{5100} = 10^{42.8}$  ergs  $\text{s}^{-1}$  at  $z = 0.1$ , very close to the flux of the lowest luminosity type-I AGNs at this redshift.<sup>3</sup> The resulting type-II sample shows a clear lack of sources at  $z \geq 0.2$ ; a behavior that has been noted in several SDSS-based publications. Given the deficiency of type-I sources at  $z \leq 0.1$ , and the incompleteness of the type-II population at  $z \geq 0.2$ , the compromise chosen here is to focus on the  $0.1 \leq z \leq 0.2$  range. In this range  $10^{42.8} \leq L_{5100} \leq 10^{44.8}$  ergs  $\text{s}^{-1}$ .

Fig. 1 compares the  $L([\text{O III}] \lambda 5007)$  distributions of the two samples in two redshift intervals, 0.1–0.15 and 0.15–0.2. There are 4197 type-II and 1331 type-I sources in the chosen luminosity and redshift ranges and the ratio is close to the expected 4:1 (note that the type-II sources are from DR4 and the type-I from DR5). The type-I sources in the histogram are all radio quiet (RQ) and are the same objects discussed in NT07. This choice is consistent with the SDSS AGN-detection algorithms that

<sup>2</sup> www.mpa-garching.mpg.de/SDSS/DR4/

<sup>3</sup> Standard cosmology with  $H_0=70$  km/sec/Mpc,  $\Omega_m = 0.3$  and  $\Omega_\Lambda = 0.7$ , is used throughout.

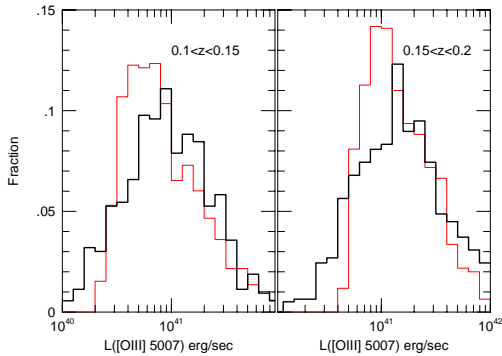


FIG. 1.—  $L([\text{O III}] \lambda 5007)$  distributions for type-I (black) and type-II (red) AGNs in two redshift intervals, as marked, using the flux limits defined in the paper.

select radio detected AGNs for spectroscopy regardless of their color. Tests show that a distribution that includes also RL sources is almost indistinguishable from the one shown here. All comparisons described below were carried out, separately, for the above two redshift bins and all show the same results. Given this, the rest of the paper addresses the entire  $0.1 \leq z \leq 0.2$  range.

The similarity of the type-I and type-II  $L([\text{O III}] \lambda 5007)$  distributions (note the shift between the two redshift bins due to the changing flux limit) suggests that they are drawn from the same parent population. The somewhat different slope at the low  $L([\text{O III}] \lambda 5007)$  end is due to the more complete type-II sample at  $z \sim 0.15$  compared with type-I AGNs that are still affected by host galaxy contamination. The small deviation on the high  $L([\text{O III}] \lambda 5007)$  side is either due to the chosen flux limit or to reddening of the  $[\text{O III}] \lambda 5007$  line. This is discussed in §4.

## 2.2. Mass and accretion rate distributions

BH masses for the modified type-II sample were obtained by applying the Tremaine et al. (2002) expression to the measured  $\sigma_*$  (e.g. Heckman et al. 2004). There are uncertainties in such mass estimates related to the host type (spheroid dominated, disk dominated, etc.). However, type-II AGNs reside almost exclusively in massive galaxies (Kauffmann et al. 2003) and the above procedure is the only one available for such sources.

For the type-I sources I used the following expression,

$$M_{\text{BH}} = 10^a L_{44}^{0.6} \left[ \frac{\text{FWHM}(H_\beta)}{1000 \text{ km s}^{-1}} \right]^2 M_\odot, \quad (2)$$

where  $L_{44} = L_{5100}/10^{44}$  ergs  $\text{s}^{-1}$  and  $a = 6.7$ . The factors in this expression are adopted from the recent work of B08 that study the *intrinsic*  $R_{\text{BLR}}$  vs.  $L_{5100}$  correlation in the K00 sample by using more accurate host galaxy subtraction. The subtraction of the host light affects the slope and the normalization of the relationship which are thus different from the ones given in K05. The best intrinsic slopes found by B08 are between 0.52 and 0.55, depending on the fitting procedure with an uncertainty of order 10%. The B08 expression cannot be used here since the values of  $L_{5100}$  are obtained from SDSS fluxes measured through the  $3''$  fibers that include the

host galaxy flux. This can be significant in low luminosity AGNs.

Eq. 2 takes the galaxy contribution into account by estimating a  $3''$  host flux for each of the B08 sources using data listed in that paper. These fluxes were added to the intrinsic B08 AGN fluxes and the best  $R_{\text{BLR}}-L_{5100}$  relationship was found by using a fitting procedure identical to the one used in that paper. The results are based on fitting only those RM sources with  $L_{5100} > 10^{42.5}$  ergs  $\text{s}^{-1}$  since these are the ones studied in the present work. The uncertainties on the slope (0.6) and the normalization ( $a$ ) are about 10% and their exact combination is of little significance over the limited luminosity range used here.

M08 suggested that radiation pressure force plays an important role in changing the velocity of BLR clouds with column density of  $\sim 10^{23} \text{ cm}^{-2}$  or smaller. In the cloud model, the column density of BLR clouds are estimated to be of this order because of various considerations involving the emitted spectrum (Netzer 1990 and references therein). For example, low ionization lines of FeII and MgII are observed to be very strong yet they cannot originate from the highly ionized, illuminated part of the clouds whose column density approaches  $10^{22} \text{ cm}^{-2}$ . Thus a more extended low ionization part of the clouds is inferred. There is no clear upper limit to the total column density, only to the part which is ionized enough to produce emission lines. The expression adopted for the present calculations is the one presented in Marconi et al. (2008b),

$$M_{\text{BH}} = 10^{a_{\text{rad}}} L_{44}^{0.5} \left[ \frac{\text{FWHM}(H_\beta)}{1000 \text{ km s}^{-1}} \right]^2 + 10^b \frac{L_{44}}{N_{23}} M_\odot, \quad (3)$$

where  $N_{23}$  is the hydrogen column density in units of  $10^{23} \text{ cm}^{-2}$ . All calculations shown below assume  $N_{23} = 1$ .

M08 analyzed a small sample of type-I AGNs with both RM-based and  $\sigma_*$ -based  $M_{\text{BH}}$ . Minimizing the scatter between the two methods they derived the following values for the virial and radiation pressure force terms:  $a_{\text{rad}} \simeq 6.13$  and  $b \simeq 7.7$ . An estimate of  $b$  can also be obtained from simple estimates of the radiation pressure force operating on BLR clouds exposed to a standard AGN continuum. This value is in good agreement with the value obtained from the minimization procedure. Note that the difference between  $a$  (Eq. 2) and  $a_{\text{rad}}$  (Eq. 3) amounts to a factor of  $\sim 4$  in  $M_{\text{BH}}$ . Most results discussed in this paper use these values and §4 addresses the possibility of a larger  $a_{\text{rad}}$ .

The above assumptions and expressions have been used to obtain  $M_{\text{BH}}$  for all sources. There is one estimate for each of the type-II sources, based on the  $M_{\text{BH}}-\sigma_*$  relationship, and two for each of the type-I sources, one that assumes Eq. 2 and one that assumes Eq. 3. The histograms of all three  $M_{\text{BH}}$  estimates are shown in Fig. 2.

I used several statistical tests to compare the histograms. Since the KS test is not very useful for comparing very large samples, I have adopted a practical alternative based on a realization procedure. It involves choosing, in a random way, a small fraction (2–10%) of the two populations and applying the KS test to the two partial samples. This was done a large number of times and the range of the resulted KS-p probability was examined. The result is a high probability that all  $M_{\text{BH}}$  dis-

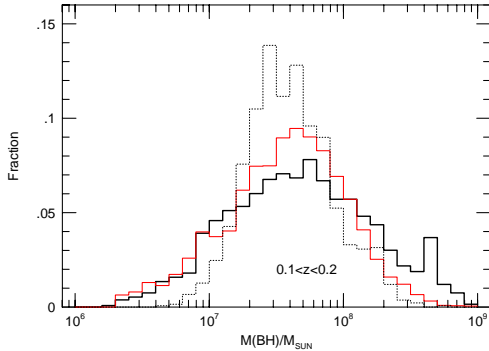


FIG. 2.—  $M_{\text{BH}}$  distributions of type-I (thick black line) and type-II (thin red line)  $0.1 \leq z \leq 0.2$  AGNs.  $M_{\text{BH}}$  estimates that include a radiation pressure force term (Eq. 3) are drawn with a dotted black line

tributions are consistent with each other. For example, when testing the virial mass estimate in type-I sources vs. the  $\sigma_*$  mass estimate in type-II sources, using 3% of the objects in each realization, I find 50% of the cases to be in the range  $0.07 \leq p \leq 0.5$ , i.e. consistent with the assumption of the same parent distribution. A very similar range of KS-p is obtained when replacing the virial assumption with the M08 assumption. I have also used the Mann-Whitney U-test, in a similar realization manner, to check for differences in the medians of the various populations. The results for the comparison of the  $M_{\text{BH}}$  distributions are similar to those of the KS test.

I have computed  $L/L_{\text{Edd}}$  for all sources where  $L$  is the bolometric luminosity. Since only  $L([\text{O III}] \lambda 5007)$  are available for estimating  $L$  in type-II sources, this was used to obtain  $L$  in type-I objects. For this purpose I assumed a simple bolometric correction factor (BC) to convert  $L_{5100}$  to  $L$  with the conversion factor given earlier (340) to convert  $L([\text{O III}] \lambda 5007)$  to  $L_{5100}$ . The factor BC is similar to the one used by Marconi et al. (2004) and various other recent publications<sup>4</sup> and the form adopted here is,

$$BC = 9 - \log L_{44} . \quad (4)$$

Fig. 3 shows three  $L/L_{\text{Edd}}$  distributions corresponding to the three  $M_{\text{BH}}$  distributions of Fig. 2. Inspection of Fig. 3 shows good agreement between the virial  $L/L_{\text{Edd}}$  distribution for type-I sources and the  $\sigma_*$   $L/L_{\text{Edd}}$  distribution for type-II sources. This is also confirmed by the KS realization tests ( $0.07 < p < 0.48$  in 50% of all realizations). The distribution of  $L/L_{\text{Edd}}$  based on Eq. 3 is clearly different showing a large peak near  $L/L_{\text{Edd}} \sim 0.1$  and almost no source close to  $L/L_{\text{Edd}} = 1$ . For example, the range  $0.05 \leq L/L_{\text{Edd}} \leq 0.2$  contains 30% of all type-I sources assuming Eq. 2 and 74% of type-I sources assuming Eq. 3. The KS realization tests confirm this result showing that 50% of all realizations produce  $10^{-4} \leq p \leq 10^{-5}$ ; i.e. extremely small probability for similar parent distributions. Unfortunately, the Mann-Whitney test is not very useful in this case since all distributions have similar mean

<sup>4</sup> Note that some recent papers, including Shen et al. (2008) and Hopkins et al. (2007), give larger bolometric corrections. This is the result of the double counting of the mid-Infrared part of the spectrum that includes mostly processed radiation.

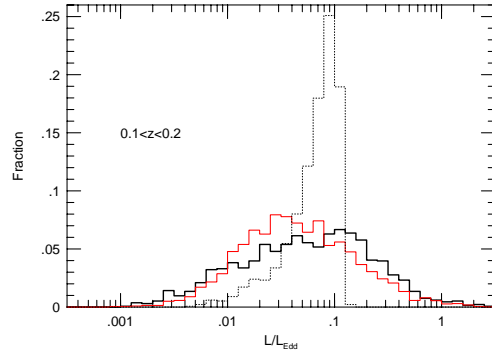


FIG. 3.—  $L/L_{\text{Edd}}$  distributions for type-I and type-II sources (symbols as in Fig. 2). Note the highly peaked distribution and the lack of large  $L/L_{\text{Edd}}$  sources when radiation pressure force is included.

$L/L_{\text{Edd}}$  (Fig. 3) despite their very different shapes.

### 3. DISCUSSION

The aim of the present paper is to investigate the mass and accretion rate distributions in AGNs hence it is crucial to understand the differences between the type-I and type-II samples. As explained in §2, the difficulties in defining two identical samples are related to the incompleteness of the type-I sample at  $z \leq 0.1$  and the deviation from a pure flux limited sample of type-II sources at  $z > 0.2$ . The chosen redshift interval of 0.1–0.2 is a compromise which is by no means perfect. For example, the matching of the two  $L([\text{O III}] \lambda 5007)$  distributions shown in the left panel of Fig. 1 ( $1 \leq z \leq 0.15$  sources) is improved if the flux limit (§2) is increased by 0.1–0.2 dex. However, there is no obvious physical reason for such an arbitrary scaling.

Reddening of the  $[\text{O III}] \lambda 5007$  line is perhaps a more plausible explanation for the differences seen in Fig. 1. This issue has been discussed extensively in Netzer et al. (2006; see §3.2) where references to earlier works are given. According to that paper, a comparison of  $L([\text{O III}] \lambda 5007)$  with  $L(2\text{--}10 \text{ keV})$  (assumes to be orientation independent) in type-I and type-II AGNs indicates more extinction in type-II sources. The typical difference is of order 0.2–0.3 dex but the number is highly uncertain since it is derived from a mixture of sources that include optically selected and X-ray selected AGNs (note that the above factor represents the *difference* in extinction, not the extinction itself which is directly measured in most type-II samples and is typically larger). More support for differences in reddening can be found in the comparison of the  $L([\text{O III}] \lambda 5007)$ -based luminosity functions of type-I and type-II AGNs (e.g. Reyes et al. 2008) and in the comparison of optical and mid-IR emission lines (Meléndez et al. 2008). Applying such a correction to the type-II sample used here brings the  $L([\text{O III}] \lambda 5007)$  distributions shown in Fig. 1 into a better agreement with the equivalent type-I distribution. The correction does not affect the type-II BH mass distribution (which is based on  $\sigma_*$ ) but increase the deduced  $L/L_{\text{Edd}}$  for type-II AGNs. This improves the (already good) agreement shown in Fig. 3.

I have also investigated the possibility that most of the

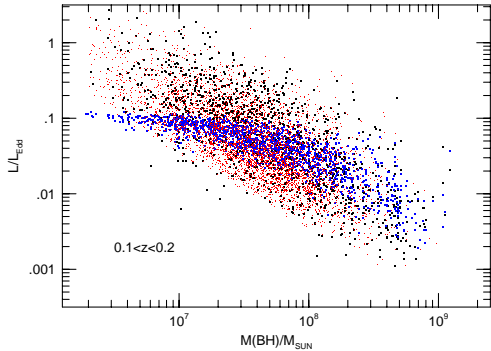


FIG. 4.—  $L/L_{\text{Edd}}$  vs.  $M_{\text{BH}}$  for type-II sources (red points) and for two assumptions about type-I sources: simple virial assumption (black points) and modified estimates (Eq. 3) that include radiation pressure force term with  $a_{\text{rad}} = 6.5$  (blue points). Note the reduced ranges in  $M_{\text{BH}}$  and  $L/L_{\text{Edd}}$  and the very different distribution compared with type-II sources, when the modified estimate is used.

differences between the two methods used to derive  $M_{\text{BH}}$  in type-I sources stem from the difference between  $a$  and  $a_{\text{rad}}$ . This is in accord with a new work by Marconi and collaborators who are studying this idea in samples of higher redshift type-I sources (A. Marconi, private communication). To test this idea I chose a larger value,  $a_{\text{rad}} = 6.5$ , in Eq. 3 and calculated new  $M_{\text{BH}}$  and  $L/L_{\text{Edd}}$  distributions. The result is a somewhat better agreement with the type-II  $M_{\text{BH}}$  distribution but the  $L/L_{\text{Edd}}$  distribution changed only slightly and shows the same typical deficiency of  $L/L_{\text{Edd}} \sim 1$  sources shown in Fig. 3. To illustrate this more clearly, I show in Fig. 4 the two dimensional distributions of  $M_{\text{BH}}$  vs.  $L/L_{\text{Edd}}$  in all three cases: one for type-II sources (red points) and two for the type-I AGNs, the virial method (black points) and the M08 expression with  $a_{\text{rad}} = 6.5$  (blue points). The very clear deviations of the Eq. 3-based estimates are evident.

Finally, I have also experimented with changing the slope in Eq. 3 to 0.6, similar to the one used in Eq. 2. This had negligible effect on the results. There are other potential complications, e.g. the possibility that the  $L([\text{O III}] \lambda 5007)/L_{5100}$  ratio is itself a function of  $L/L_{\text{Edd}}$ , the suggestion that the bolometric correction factor, BC, depends on  $L/L_{\text{Edd}}$ , and more. The data used here do not support the first and there is no information to test the latter.

The main result of the present work is the significantly different  $L/L_{\text{Edd}}$  distribution of low luminosity low redshift type-I AGNs compared with type-II sources under the assumption that radiation pressure force plays an important role in affecting the BLR gas velocity. The differences almost completely disappear when a “standard” virial mass estimate (Eq. 2) is used. Eq. 3 shows that the radiation pressure force term is negligible if the column densities of the  $\text{H}\beta$  producing BLR clouds are significantly larger than  $10^{23} \text{ cm}^{-2}$ , perhaps as large as  $10^{24} \text{ cm}^{-2}$ . Radiation pressure force bounds to have some effect on optically thick gas thus the results shown here can be viewed as an indication for large column density BLR clouds. As explained, all this relates only to the cloud model of the BLR.

The existence of extremely large column density clouds

can change some aspects of present AGN models. For example, it limits the possibility of escaping BLR gas and increases the chance of eventual accretion onto the central BH. It also suggests a large column of neutral gas at the back of such clouds and a more hospitable environment for molecules and dust formation and survival. The physical scale of the clouds must be larger too compared with previous estimates with possible implications for cloud-cloud collisions. Regarding high redshift sources, the Marconi et al. (2008b) mass calculations is based on the observation of the  $\text{C IV } \lambda 1549$  line. Since the column densities of  $\text{H}\beta$  producing and  $\text{C IV } \lambda 1549$  producing clouds are not necessarily the same (e.g. Kaspi and Netzer 1999) this would complicate the comparison with low redshift samples.

Finally, the present work applies to AGNs with  $10^{42.8} \leq L_{5100} \leq 10^{44.8} \text{ ergs s}^{-1}$  in the 0.1–0.2 redshift interval. I have also tested the  $L/L_{\text{Edd}}$  distribution in somewhat higher luminosity higher redshift ( $\sim 0.25$ ) type-II sources from the DR4 archive. I found several cases with  $L/L_{\text{Edd}} \sim 1$ , beyond the limit obtained by using Eq. 3. As for a similar test for higher redshift, more luminous sources, the situation is less clear. First it is hard to find overlapping type-I and type-II samples where a similar analysis can be applied. Moreover, the applicability of the  $M_{\text{BH}}-\sigma_*$  relationship has only been demonstrated at low redshift. The current understanding of the co-evolution of massive BHs and their hosts at high redshift does not allow such a test at the present time.

I am grateful to Alessandro Marconi, Benny Trakhtenbrot and Guinevere Kauffmann for useful discussions. Funding for this work has been provided by the Israel Science Foundation grant 364/07.

Funding for the SDSS and SDSS-II has been provided by the Alfred P. Sloan Foundation, the Participating Institutions, the National Science Foundation, the U.S. Department of Energy, the National Aeronautics and Space Administration, the Japanese Monbukagakusho, the Max Planck Society, and the Higher Education Funding Council for England. The SDSS Web Site is <http://www.sdss.org/>.

The SDSS is managed by the Astrophysical Research Consortium for the Participating Institutions. The Participating Institutions are the American Museum of Natural History, Astrophysical Institute Potsdam, University of Basel, University of Cambridge, Case Western Reserve University, University of Chicago, Drexel University, Fermilab, the Institute for Advanced Study, the Japan Participation Group, Johns Hopkins University, the Joint Institute for Nuclear Astrophysics, the Kavli Institute for Particle Astrophysics and Cosmology, the Korean Scientist Group, the Chinese Academy of Sciences (LAMOST), Los Alamos National Laboratory, the Max-Planck-Institute for Astronomy (MPIA), the Max-Planck-Institute for Astrophysics (MPA), New Mexico State University, Ohio State University, University of Pittsburgh, University of Portsmouth, Princeton University, the United States Naval Observatory, and the University of Washington.

## REFERENCES

- Baldwin, J., Ferland, G., Korista, K., & Verner, D. 1995, ApJ, 455, L119
- Adelman-McCarthy, et al., 2006, ApJS, 162, 38.
- Bentz, M., Peterson, B.M., Netzer, H., Pogge, R.W., & Vestergaard, M., 2008 (submitted to ApJ)
- Elitzur, M., & Shlosman, I. 2006, ApJ, 648, L101
- Everett, J. E. 2005, ApJ, 631, 689
- Groves, B., Kewley, L., Kauffmann, G., & Heckman, T. 2006, New Astronomy Review, 50, 743
- Heckman, T. M., Kauffmann, G., Brinchmann, J., Charlot, S., Tremonti, C., & White, S. D. M. 2004, ApJ, 613, 109
- Korista, K., Baldwin, J., Ferland, G., & Verner, D. 1997, ApJS, 108, 401
- Hopkins, P. F., Richards, G and Humanist, L, 2007, ApJ654, 731
- Kaspi, S., & Netzer, H. 1999, ApJ, 524, 71
- Kaspi, S., Smith, P. S., Netzer, H., Maoz, D., Jannuzi, B. T., & Giveon, U. 2000, ApJ, 533, 631 (K00)
- Kaspi, S., Maoz, D., Netzer, H., Peterson, B. M., Vestergaard, M., & Jannuzi, B. T. 2005, ApJ, 629, 61 (K05)
- Kauffmann, G., et al. 2003, MNRAS, 346, 1055
- Marconi, A., Risaliti, G., Gilli, R., Hunt, L. K., Maiolino, R., & Salvati, M. 2004, MNRAS, 351, 169
- Marconi, A., Axon, D. J., Maiolino, R., Nagao, T., Pastorini, G., Pietrini, P., Robinson, A., & Torricelli, G. 2008a, ApJ, 678, 693, (M08)
- Marconi, A., Axon, D., Maiolino, R., Nagao, T., Pietrini, P., Robinson, A., & Torricelli, G. 2008b, arXiv:0809.0390
- Meléndez, M., et al. 2008, ApJ, 682, 94 & Torricelli, G. 2008b, arXiv:0809.0390
- Netzer, H., 1990, in *Active Galactic Nuclei*, SAAS-FEE advanced course 20
- Netzer, H., & Trakhtenbrot, B. 2007, ApJ, 654, 754 (NT07)
- Netzer, H., Mainieri, V., Rosati, P., & Trakhtenbrot, B. 2006, A&A, 453, 525
- Onken, C. A., & Peterson, B. M. 2002, ApJ, 572, 746
- Peterson, B. M., & Bentz, M. C. 2006, New Astronomy Review, 50, 796
- Reyes, R., et al. 2008, arXiv:0801.1115
- Shen, Y., Greene, J. E., Strauss, M. A., Richards, G. T., & Schneider, D. P. 2008, ApJ, 680, 169
- Tremaine, S., et al. 2002, ApJ, 574, 740
- Vestergaard, M., & Peterson, B. M. 2006, ApJ, 641, 689
- York, et al., 2000, AJ, 120, 1579
- Zakamska, N. L., et al. 2003, AJ, 126, 2125